



## Microstructure and magnetic properties of as-quenched and heat-treated (Nd,Dy)FeB powders produced by high pressure gas atomization

J. E. Snyder, C. C. H. Lo, X. Fang, B. Kriegermeier, and D. C. Jiles

Citation: [Journal of Applied Physics](#) **85**, 5678 (1999); doi: 10.1063/1.369838

View online: <http://dx.doi.org/10.1063/1.369838>

View Table of Contents: <http://scitation.aip.org/content/aip/journal/jap/85/8?ver=pdfcov>

Published by the [AIP Publishing](#)

---

### Articles you may be interested in

[Magnetic properties and microstructure of Nd-Fe-B sintered magnets with DyHx addition](#)

J. Appl. Phys. **111**, 07A705 (2012); 10.1063/1.3671426

[A high-resolution field-emission-gun, scanning electron microscope investigation of anisotropic hydrogen decrepitation in Nd-Fe-B-based sintered magnets](#)

J. Appl. Phys. **107**, 09A742 (2010); 10.1063/1.3348632

[Effect of heat treatment on microstructure and magnetic properties of anisotropic Nd-Fe-B films with Mo or Ti buffer layer](#)

J. Appl. Phys. **98**, 113905 (2005); 10.1063/1.2136208

[Magnetic properties and microstructure of LaCo 5 -based powders produced by mechanical milling and subsequent annealing](#)

J. Appl. Phys. **91**, 6147 (2002); 10.1063/1.1467628

[The magnetic properties of Nd-Fe-B powders produced by mechanical grinding in hydrogen atmosphere](#)

J. Appl. Phys. **85**, 5687 (1999); 10.1063/1.369841

---



**AIP** | Journal of  
Applied Physics

*Journal of Applied Physics* is pleased to  
announce **André Anders** as its new Editor-in-Chief

# Microstructure and magnetic properties of as-quenched and heat-treated (Nd,Dy)FeB powders produced by high pressure gas atomization

J. E. Snyder,<sup>a)</sup> C. C. H. Lo, X. Fang, B. Kriegermeier, and D. C. Jiles

Ames Laboratory, Iowa State University, Ames, Iowa 50011

The magnetic properties and microstructures of a series of as-quenched and heat-treated inert gas atomized (IGA) rare-earth rich (Nd,Dy)–Fe–B particles have been investigated. Heat treatment was found to substantially improve magnetic properties, with effects most pronounced in samples with higher Dy content and higher total rare earth (RE) content. The as-quenched particles consisted of an underquenched dendritic-like structure with the majority phase  $\text{RE}_2\text{Fe}_{14}\text{B}$ , and a fine network of RE-rich material between the grains. The heat-treated particles showed a change in microstructure which correlated with magnetic property changes. Particles which showed little change in magnetic properties showed no obvious change in microstructure. Particles which showed large changes in magnetic properties showed a large change in microstructure: most of the fine network of RE-rich interdendritic material disappeared, leaving behind only a few small isolated regions. This would seem to indicate that the predominant mechanism determining coercivity in these IGA RE-rich (Nd,Dy)–Fe–B powders is nucleation of reverse domains, rather than domain wall pinning at nonmagnetic intergranular material. © 1999 American Institute of Physics. [S0021-8979(99)44708-5]

Following the discovery of Nd–Fe–B permanent magnet material in 1983,<sup>1,2</sup> much of the interest in producing Nd–Fe–B magnets centered on one of two processes: a powder metallurgy approach which employs alloying, crushing, pressing in a magnetic alignment field, sintering, and heat treatment,<sup>2,3</sup> and a rapid solidification melt-spinning process followed by mechanical grinding, hot-pressing, and hot working (die upsetting).<sup>3,4</sup>

In recent years, inert-gas atomization (IGA) has been proposed as an alternate method of producing Nd–Fe–B powder.<sup>5,6</sup> IGA is also a rapid-quench process ( $10^4$  to  $10^5$  K/s),<sup>5</sup> and has several potential advantages: The power is produced directly from the melt, in a simpler, more-economical process. The particles are magnetically isotropic spheres, ranging from 1–150  $\mu\text{m}$  diameter. The spherical shape offers superior flowability and packing for the production of isotropic bonded and hot-pressed magnets, the fastest growing areas of the permanent magnet market.<sup>7</sup>

However, because melt-spinning and IGA differ in cooling rate ( $10^5$ – $10^7$  versus  $10^4$ – $10^5$  K/s, respectively),<sup>8</sup> the same melt composition could not be used for both. The lower cooling rate of IGA caused  $\alpha$ -Fe precipitation, and hence a lower energy product.<sup>6</sup> Several methods have been employed to prevent  $\alpha$ -Fe precipitation: A rare-earth (RE)-rich melt can be used. Or, alternatively, Ti and C can be added to the melt to change its solidification characteristics.<sup>6</sup> The current study employed the former method.

The starting materials for this study were prepared from commercial grade powders by induction melting. Compositions were checked by inductive coupled plasma techniques. All the samples were fabricated with RE-rich composition compared to stoichiometric  $\text{RE}_2\text{Fe}_{14}\text{B}$  (see Table I). Two different total RE percentages were tried, and in two of the samples,  $\sim 3$  wt % Dy was substituted for Nd. The RE–Fe–B

particles were then prepared by IGA, with a close coupled annular feed atomizer, using He gas (further details are outlined in Ref. 5).

The RE–Fe–B particles were sieved in air; 50–75  $\mu\text{m}$  diam particles were used for this study. Half of each sample was saved as-quenched. The other half was heat treated, which consisted of heating in vacuum at 120 °C/min to 650 °C, holding there for 10 min, then cooling in the water-cooled furnace. This heat treatment had been optimized by previous experiments in which 50–75  $\mu\text{m}$  diam particles were heat treated at different temperatures spanning the range of 500–900 °C by 25 or 50 °C increments. Optimum temperature was then chosen to maximize the energy product. All the alloys of this study had the same optimum heat treatment, 650 °C.<sup>9</sup>

As-quenched and heat-treated samples were each mounted in epoxy for magnetic property measurement and microstructure observation. Magnetic hysteresis loops were measured by vibrating sample magnetometer (VSM), with a maximum applied field of 26.5 kOe. No demagnetization corrections were applied. For scanning electron microscope (SEM) observation, each sample was mounted and polished to reveal the cross section, then coated with a thin layer of Au. An Amray field emission SEM was used, operating at 15 kV. The particles were imaged in the backscattered electron

TABLE I. Compositions of IGA RE–Fe–B powders.

Sample No.	Dy (wt %)	Nd (wt %)	Fe (wt %)	B (wt %)	Total rare-earth content (wt %)
1 and 2	0.1	33.4	65.4	1.1	33.5
3 and 4	0.3	35.3	63.3	1.1	35.6
5 and 6	2.8	32.4	63.7	1.1	35.2
7 and 8	2.9	30.7	65.2	1.1	33.6
Stoichiometric $\text{Nd}_2\text{Fe}_{14}\text{B}$	—	22.4	76.5	1.1	22.4

<sup>a)</sup>Electronic mail: jesnyder@iastate.edu

TABLE II. Magnetic properties of IGA RE-Fe-B powders.

Sample No.	Dy content (wt %)	Heat treatment <sup>a</sup>	Total rare-earth content (wt %)	Coercivity $H_{ci}$ (Oe)	Remanence $M_r$ (emu/g)
1	0.1	AQ	33.5	2700	36.2
2	0.1	HT	33.5	4370	34.6
3	0.3	AQ	35.6	1660	24.6
4	0.3	HT	35.6	5670	34.0
5	2.8	AQ	35.2	990	17.6
6	2.8	HT	35.2	12 390	52.2
7	2.9	AQ	33.6	4510	38.8
8	2.9	HT	33.6	8900	45.6

<sup>a</sup>AQ: as quenched; HT: heat treated.

mode, in which the observed contrast arises from variations in composition. Chemical composition of different regions of the particles was determined by energy-dispersive x-ray (EDX) analysis, with a spatial resolution of  $\sim 0.8 \mu\text{m}$ .

In order to ascertain what effect the packing fraction of particles in the epoxy had on the magnetic measurements, a series of samples was prepared using the same powder (composition of sample 5 in Table I, sieved for less than  $100 \mu\text{m}$ ; heat treated at  $750^\circ\text{C}$  for 10 min). Samples were prepared with particle volume fractions 0.25, 0.30, 0.35, 0.40, and 0.50, and cut into cylinders 4 mm diameter by 5 mm tall.

Measured coercivity  $H_{ci}$  and remanence  $M_r$  data are shown in Table II. For comparison purposes, one can think of the sample set as divided three different ways: There are as-quenched samples (1, 3, 5, and 7) and heat-treated samples (2, 4, 6, and 8). There are samples with low Dy content (samples 1, 2, 3, and 4) and samples with higher Dy content (5, 6, 7, and 8). There are samples with lower total RE content (samples 1, 2, 7, and 8) and samples with higher total RE content (3, 4, 5, and 6).

First let us consider the coercivity  $H_{ci}$  data. Comparing as-quenched to heat-treated samples (by pairs, comparing 1 and 2, 3 and 4,...), one can see that the heat treatment causes a considerable increase in  $H_{ci}$ . If one further compares the high Dy samples (samples 5, 6, 7, and 8) and the low Dy samples (samples 1, 2, 3, and 4) one can see that there is a greater increase in  $H_{ci}$  with heat treatment for the high Dy samples. Furthermore, if within each Dy content group, one compares the high total RE samples to the low total RE samples (i.e., compare samples 3 and 4 to 1 and 2; and compare samples 5 and 6 to 7 and 8), one can see that the high total RE samples show the greatest increase in  $H_{ci}$ . Thus the heat treatment causes an improvement in  $H_{ci}$ , with the largest increase in samples with higher Dy content and higher total RE content.

Now consider the remanence  $M_r$  data. Comparing as-quenched to heat-treated samples (by pairs, comparing 1 and 2, 3 and 4,...), one can see that other than the 1–2 pair which have essentially the same  $M_r$ , the heat treatment causes a substantial improvement in  $M_r$ . Comparing the high total RE samples (samples 3, 4, 5, and 6) and the low total RE samples (samples 1, 2, 7, and 8), one can see that there is a greater increase in  $M_r$  in the samples with higher RE con-

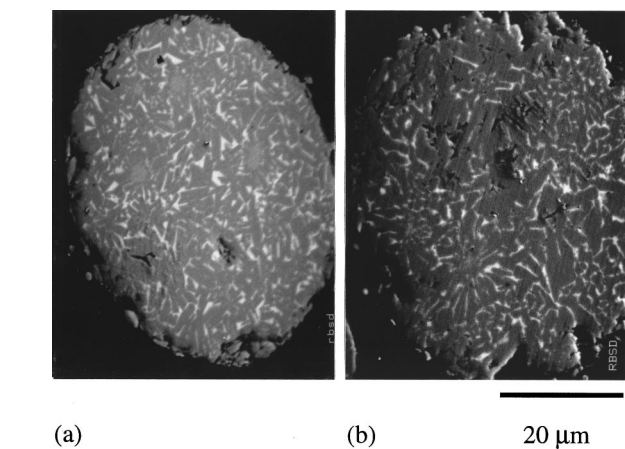


FIG. 1. SEM micrographs of: (a) sample 3 (as quenched, 0.3% Dy) and (b) sample 4 (heat treated, 0.3% Dy).

tent. If one further compares the high Dy samples to the low Dy samples within each RE-content group, (i.e., compare samples 7 and 8 to 1 and 2; and compare samples 5 and 6 to 3 and 4), one can see that the high Dy samples show the greatest increase in  $M_r$ . Thus the heat treatment can cause an improvement in  $M_r$ , with the largest increase observed in samples with higher total RE content and higher Dy content.

The measurements of  $H_{ci}$  as a function of packing fraction were a constant  $10.17 \text{ kOe}$  to within  $\pm 1.7\%$ . The measurements of  $M_r$  as a function of packing fraction were a constant  $54.0 \text{ emu/g}$  to within  $\pm 2.5\%$ . Thus it appears that the important interactions determining  $H_{ci}$  and  $M_r$  take place within the particles, rather than between the particles.

In order to investigate the mechanisms determining  $H_{ci}$  and  $M_r$  and their increase with heat treatment, polished cross sections were examined by SEM in backscattering electron mode and by EDX compositional analysis. Representative micrographs are shown in Figs. 1 and 2. Since microstructure can depend on quench rate in IGA powders and quench rate depends on particle size,<sup>6</sup> particles of the same approximate size ( $60 \mu\text{m}$  diameter) were compared. The microstructures of all the particles consist of two phases: The grey majority phase is identified by EDX as being  $\text{RE}_2\text{Fe}_{14}\text{B}$ . The white

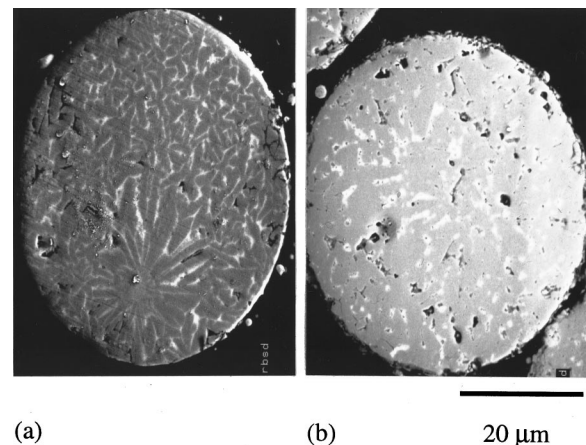


FIG. 2. SEM micrographs of: (a) sample 5 (as quenched, 2.8% Dy) and (b) sample 6 (heat treated, 2.8% Dy).

regions inbetween consist of RE-rich material, which by EDX measures at between 28 and 88 at % Nd. This variation could be due, at least in part, to the difficulty in determining whether the activated volume for the EDX measurement lies entirely within the white region.

First consider the micrographs of the as-quenched particles: Fig. 1(a) (sample 3) and Fig. 2(a) (sample 5). Both show a dendritic-like microstructure of grey  $\text{RE}_2\text{Fe}_{14}\text{B}$  phase with typical feature size approximately  $5\text{ }\mu\text{m}$  by  $1\text{ }\mu\text{m}$ . In between these features is a fine network of white RE-rich regions. This microstructure is indicative of the underquenched regime (i.e., particles are entirely crystalline, microstructure is dendritic, grains are relatively large). For this size RE-Fe-B particle, IGA could be expected to produce underquenched particles.<sup>6</sup>

Now consider the heat-treated particles: Fig. 1(b) (sample 4) and Fig. 2(b) (sample 6). In the sample with the lower Dy content [Fig. 1(b)], the microstructure does not appear to have changed substantially. In the sample with the higher Dy content [Fig. 2(b)], the heat treatment has caused most of the fine structure of white RE-rich regions to disappear, leaving only isolated small white regions, and a much larger area of uniform grey. It would appear that the RE-rich material has dissolved into the majority phase. One can make similar observations concerning the other low Dy and high Dy samples (samples 1 and 2, and 7 and 8, respectively). There are known differences in the Nd-Fe and Dy-Fe binary phase diagrams,<sup>10</sup> and in melt-spun ribbons, the crystallization temperature of Dy-Fe-B is known to be  $120^\circ\text{C}$  higher than Nd-Fe-B.<sup>11</sup> It would appear that in the present system, the addition of Dy changes the chemistry or kinetics enough to facilitate the observed differences of change in microstructure with heat treatment.

With melt-spun ribbons, heat treatment of underquenched RE-Fe-B does not cause significant improvement of magnetic properties.<sup>6</sup> However, for the underquenched IGA powders of the present study, considerable improvement in  $H_{ci}$  and  $M_r$  is observed. This effect has also been observed by several other researchers.<sup>5,6</sup> One proposed explanation for magnetic property improvement in similar powder samples, is the reaction of  $\alpha$ -Fe precipitates during heat treatment.<sup>5</sup> In the present work,  $\alpha$ -Fe precipitates such as those shown in Ref. 6 are not observed. Rather, it appears that the major microstructural change observed by SEM is the disappearance or dissolution of the fine network of RE-rich material in the samples with high Dy content. This appears to correlate with  $H_{ci}$  and  $M_r$  changes: The larger the magnetic property changes that are observed, the larger the observed disappearance of the fine network of RE-rich material.

It is generally agreed that in sintered  $\text{Nd}_2\text{Fe}_{14}\text{B}$ , the mechanism determining  $H_{ci}$  is the nucleation of reverse domains.<sup>12</sup> However, for  $\text{Nd}_2\text{Fe}_{14}\text{B}$  magnets produced by melt spinning and die upsetting, there has apparently been some controversy as to whether the predominant mechanism is nucleation of reverse domains, or domain wall pinning by nonmagnetic material between grains.<sup>13</sup> It appears that there has not been much work addressing the mechanism determining  $H_{ci}$  in RE-rich IGA powders. For the samples in the

present study, it would appear that nucleation of reverse domains would be the predominant mechanism determining  $H_{ci}$ , since with heat treatment,  $H_{ci}$  goes up while most of the network of RE-rich material between the grains disappears. This question could be addressed more completely by measurements of initial magnetization curves or  $H_{ci}$  as a function of maximum applied field.<sup>13</sup> Understanding the predominant mechanism determining  $H_{ci}$  in IGA RE-Fe-B powders is important in order to optimize their performance for permanent magnet applications.

In conclusion, the magnetic properties and microstructures of a series of as-quenched and heat-treated IGA RE-rich (Nd,Dy)-Fe-B powders have been investigated. The heat treatment substantially improved coercivity and remanence, with the effects most pronounced in samples with higher Dy content and higher total RE content. The as-quenched particles consisted of an underquenched dendritic-like structure, with the majority phase  $\text{RE}_2\text{Fe}_{14}\text{B}$ , and a fine network of RE-rich material between the grains. The heat-treated particles showed a change in microstructure which correlated with magnetic property changes. Particles which showed little change in magnetic properties showed no obvious change in microstructure. Particles which showed large changes in magnetic properties showed a large change in microstructure: most of the fine network of RE-rich interdendritic material disappeared, leaving behind only a few small isolated regions. This would seem to indicate that the predominant mechanism determining coercivity in these IGA RE-rich (Nd,Dy)-Fe-B powders is nucleation of reverse domains, rather than domain wall pinning at nonmagnetic intergranular material.

The Ames Laboratory is operated by the U.S. Department of Energy (DOE) by Iowa State University under Contract No. W-7405-ENG-82. This work was supported by the U.S. Department of Energy, Office of Basic Energy Sciences, and the Office of Basic Energy Sciences Center for Excellence in Synthesis and Processing, Program on Tailored Microstructures in Hard Magnets. The authors wish to thank D. J. Branagan of the Idaho National Engineering Laboratory for providing the RE-Fe-B powders, and F. Laabs of Ames Laboratory for his help on the SEM work.

<sup>1</sup>N. C. Koon and B. D. Das, J. Appl. Phys. **55**, 2063 (1984).

<sup>2</sup>M. Sagawa, S. Fujimura, N. Togawa, H. Yamamoto, and Y. Matsuura, J. Appl. Phys. **55**, 2083 (1984).

<sup>3</sup>N. Yoshikawa, Y. Kasai, T. Watanabe, and S. Shibata, J. Appl. Phys. **69**, 6049 (1991).

<sup>4</sup>R. W. Lee, Appl. Phys. Lett. **46**, 790 (1985).

<sup>5</sup>L. H. Lewis, C. H. Sellers, and V. Panchanathan, IEEE Trans. Magn. **32**, 4371 (1996).

<sup>6</sup>C. H. Sellers, D. J. Branagan, T. A. Hyde, L. H. Lewis, and V. Panchanathan, in *Proceedings of the 14th International Workshop on Rare-Earth Magnets and Their Applications*, edited by F. P. Missell, V. Villas-Boas, H. R. Rechenberg, and F. J. G. Landgraf (World Scientific, Singapore, 1996).

<sup>7</sup>C. H. Sellers, Mat. Tech. **11**, 219 (1996).

<sup>8</sup>S. J. Savage and F. H. Froes, J. Met. **36**, 20 (1984).

<sup>9</sup>D. J. Branagan (personal communication).

<sup>10</sup>*Binary Alloy Phase Diagrams*, 2nd ed., edited by T. B. Massalski (ASM International, Materials Park, OH, 1990).

<sup>11</sup>Y. F. Tao and G. C. Hadjipanayis, J. Appl. Phys. **57**, 4103 (1985).

<sup>12</sup>J. F. Herbst and J. J. Croat, J. Magn. Mater. **100**, 57 (1991).

<sup>13</sup>L. H. Lewis, Y. Zhu, and D. O. Welch, J. Appl. Phys. **76**, 6235 (1994).